

# Altered sensory filtering and coding properties by synaptic dynamics in the electric sense

Krisztina Szalisznyó<sup>a,b,c,\*</sup>, André Longtin<sup>a,b</sup>, Leonard Maler<sup>b</sup>

<sup>a</sup>Physics Department, University of Ottawa, 150 Louis Pasteur, Ottawa, Ont., Canada K1N 6N5

<sup>b</sup>Department of Cellular and Molecular Medicine, University of Ottawa, 451 Smyth Road, Ottawa, Ont., Canada K1H 8M5

<sup>c</sup>Department of Biophysics, KFKI Research Institute of the Hungarian Academy of Sciences, H-1525 P.O. Box 49, Budapest, Hungary

Available online 13 February 2006

## Abstract

This modeling study examines the short-term synaptic plasticity properties of the electrosensory lateral lobe (ELL) afferent pathway in the weakly electric fish, *Apteronotus leptorhynchus*. We studied the possible functional consequences of a simple phenomenological model of synaptic depression by taking into consideration the available in vivo and in vitro results [N. Berman, L. Maler, Inhibition evoked from primary afferents in the electrosensory lateral line lobe of the weakly electric fish (*Apteronotus leptorhynchus*), *J. Neurophysiol.* 80(6) (1998) 3173–3196; M.J. Chacron, B. Doiron, L. Maler, A. Longtin, J. Bastian, Non-classical receptive field mediates switch in a sensory neuron's frequency tuning, *Nature* 26(424) (2003) 1018–1022]. Filtering and coding properties were examined. We find that simple short-term phenomenological synaptic depression can change steady-state filtering properties and explain how the known physiological constraints influence the coding capabilities of the ELL pyramidal cells via dynamic synaptic transmission.

© 2006 Elsevier B.V. All rights reserved.

**Keywords:** Short-term synaptic dynamics; Neural coding; Neural filtering; Synaptic depression; Electric fish; Electroreception; ELL

## 1. Introduction

The objective of this research is to understand the synaptic plasticity properties between the primary electrosensory afferents and sensory pyramidal cells in the afferent pathway of the weakly electric fish. Pyramidal cells in the electrosensory lateral lobe (ELL) receive multiple convergent mono-synaptic excitatory and disynaptic inhibitory inputs from the primary electrosensory afferents (P units). These afferents carry information about the amplitude modulated quasi-sinusoidal electric organ discharge (EOD) and are able to transmit signals with high fidelity over frequencies ranging from low to very high values [1]. Here, we studied the effect of short-term synaptic plasticity on coding and filtering of time varying signals. In vitro studies from the ELL have demonstrated

that these P-unit synapses show both short-term facilitation and depression; the biophysical substrates of this plasticity are unknown and it is possible that the depressive component involves postsynaptic inhibition as well as mechanisms intrinsic to the synapses [2]. We focus here on the depressive component since, over longer time scales, it predominates over facilitation. We employed computational models incorporating the key known physiological properties of the synapse and the postsynaptic pyramidal cells. Our strategy was to constrain the P-unit-to-pyramidal cell synaptic properties based on in vitro data from electric fish [2] as well as on the time constants of synaptic depression in similar auditory brainstem systems [6,13]. We then quantitatively varied the synaptic time constants to determine what dynamics could support the frequency filtering seen in vivo.

## 2. Methods: mathematical model

A modulated Poisson process is given as an input to a pyramidal cell model with synaptic depression. This input

\*Corresponding author. Department of Biophysics, KFKI Research Institute of the Hungarian Academy of Sciences, H-1525 P.O. Box 49, Budapest, Hungary. Tel.: +36 1 3959220x1238; fax: +36 1 3959151.

E-mail address: [szali@sunserv.kfki.hu](mailto:szali@sunserv.kfki.hu) (K. Szalisznyó).

is meant to mimic the signal received from the electroreceptor afferents, which encodes amplitude modulations of the EOD. Two sets of simulations were performed. In order to study filtering properties, sinusoidally modulated (SAM) Poisson inputs were generated. In these simulations, we changed the sinusoidal modulation frequency of the mean rate parameter of the Poisson input. Secondly, we designed simulations with the aim of determining coding properties. For these purposes low-pass filtered Gaussian noise was used as a time-dependent rate parameter for Poisson spike generation. In both cases, these input spike trains drove a leaky integrate-and-fire neuron (LIF) via a phenomenological synaptic depression model. Computer simulations were performed on a laptop (Clevo 5620D 2GHz Pentium-IV), using Fortran-77 language on a Debian Linux (kernel version 2.0.34) platform. For the computation of filtering and coding properties, we used MatLab 6.5 software running under Windows-XP platform on the same machine. The Euler integration method was used with an integration time step of 0.025 ms.

### 2.1. Poisson input modulated by sinusoids and by low-pass filtered Gaussian noise

The mean rate parameter  $\lambda$  of the Poisson input was modulated according to:

$$\lambda(t) = A + M \sin(2\pi ft), \quad (1)$$

where  $M$  is the modulation depth,  $f$  is the modulation frequency, and  $A$  is an additive constant term (which determines the mean rate without SAM). We looked at the effect of varying  $f$  in order to approximate the frequency filtering properties of the synaptic dynamics. Bode plots (gain-vs-frequency) for SAM Poisson input were computed from the steady-state responses of the system.

To examine the coding properties of our model, low-pass filtered Gaussian noise was generated and then we considered a doubly stochastic Poisson process, where the rate of occurrence  $\lambda(t)$  was the low-pass filtered Gaussian noise. We constructed this process in order to mimic the physiologically plausible environmental input of the ELL pyramidal cells. Gaussian white noise was generated by using the Box–Muller algorithm and we have used a fourth order filter to low-pass filter the noise. The cutoff angular frequency was chosen to be 120 Hz because this (0–120 Hz) regime corresponds well with the environmentally plausible AM modulation range of the EOD. The low-pass filtered noise was multiplied by a scalar ( $q = 0.125$ ) in order to adjust the physiologically realistic presynaptic input rate.

### 2.2. Synaptic depression model

The model of synaptic depression used in our study has been described in [5]. The variable  $D$  denotes the recovery from synaptic depression. Between input spikes, it evolves

according to the following equation:

$$\frac{dD}{dt} = \frac{1-D}{\tau_d}. \quad (2)$$

The  $G$  variable is the synaptic conductance, which is governed by

$$\frac{dG}{dt} = \frac{-G}{\tau_g}. \quad (3)$$

At every incoming spike in the modulated Poisson input, the depression variable is updated as  $D \rightarrow Dd$  where  $d$  is a constant factor. Likewise, the synaptic conductance  $G$  gets updated according to  $G \rightarrow G + Dg$  where  $g$  is a constant factor. In our simulations we used  $d = 0.3$  and  $g = 0.2$ .

### 2.3. Leaky integrate and fire neuron

The leaky integrate and fire model is described by the following equation:

$$\frac{dV}{dt} = \frac{-V}{\tau_m} + \frac{I_{\text{syn}}}{C} + \frac{I_{\text{inj}}}{C}, \quad (4)$$

$$I_{\text{syn}} = g_{\text{max}} G(V - E_{\text{syn}}), \quad (5)$$

where  $V$  is the membrane potential,  $\tau_m$  is the membrane time constant and  $C$  is the membrane capacitance. When  $V$  reaches threshold we reset the membrane to  $V_{\text{reset}}$ . The following parameters are used:  $\tau_m = 10$  ms,  $E_{\text{syn}} = 0$  mV,  $C = 1$  nF,  $V_{\text{reset}} = -80$  mV,  $V_{\text{thres}} = -55$  mV,  $g_{\text{max}} = 0.2$ ,  $A = 0.2$ ,  $M = 0.2$ . For the firing rate drop compensation, the following DC currents were used: ( $I_{\text{inj}} = 0.25, 0.57, 0.805, 1.14, 1.37$ ) for ( $\tau_g = 20, 17.5, 15, 12.5, 10$  ms), and ( $I_{\text{inj}} = 1.05, 0.95, 0.805, 0.65, 0.5$ ) for ( $\tau_d = 20, 17.5, 15, 12.5, 10$  ms), respectively.

We performed two sets of simulations. (A): We let the firing rate change as we altered the synaptic dynamics parameters. In these simulations  $I_{\text{inj}}$  was zero; unless the synaptic (noisy) input is present, the LIF neuron does not fire. (B): The LIF firing rate was kept constant (72 Hz) by adjusting the values of bias current ( $I_{\text{inj}}$ ) while changing the synaptic depression parameters. This allowed us to follow the changes in coding properties without the effect of the firing rate drop [11].

## 3. Model performance analysis

### 3.1. Quantification of filtering properties

In order to study filtering properties, SAM Poisson input drives the synapses and the postsynaptic LIF neuron according to the equations described in the previous section. In all of the simulations where we studied the filtering properties, we used the A-type simulations (see Methods) where the input injected current  $I_{\text{inj}}$  was set to zero. For each modulation frequency, we numerically constructed the rate histogram from the LIF spike train outputs, and compared its modulation to that of the input

spiketrain histogram as in [9]. The total simulation duration was 200 s independent of the stimulus frequency. This simulation duration was long enough to average out the effect of the initial transients in the solutions. Cycles were collected for computing input output cycle histograms which were then fitted by sinusoids in order to calculate gain values for each given input frequency. Before the fitting, the mean values of the cycle histograms were subtracted from the histograms at all modulation frequencies. Fits were performed by a nonlinear fitting algorithm provided in the MatLab Statistics toolbox using least-square data fitting by the Gauss–Newton method. The gain of the response at each SAM stimulus was computed by dividing the amplitudes of the fitted sinusoids of the input and output cycle histograms.

### 3.2. Quantification of coding ability

In order to quantify the information transmission ability of the synapse and the postsynaptic neuron, coherence, mutual information and coding fraction measures were used. All the simulations were 300 s long which is long enough for stimulus estimation and mutual information calculation by indirect method [7]. We followed how the coherence measure changed with synaptic dynamic parameters. The coherence function  $C_{A,B}$  was calculated according to

$$C_{A,B} = \frac{[X_{A,B}(f)]^2}{S_{A,B}(f)S_{st}(f)}, \quad (6)$$

where  $X_{A,B}$ ,  $S_{A,B}$  are, respectively, the cross-spectrum between the spike train and the signal, and the power spectrum of the output spike train in the presence of the input stimulus.  $S_{st}(f)$  is the power spectrum of the input stimulus. For Gaussian input, a lower bound on the mutual information (MI) rate can be calculated from the coherence function according to [10]

$$M_{A,B} = - \int_0^{cf} \log_2[1 - C_{A,B}(f)] df, \quad (7)$$

where cf is the input cutoff frequency. We employed this measure in order to calculate the transmitted information per spike, since altering synaptic dynamics changes the synaptic conductance and therefore the overall injected current—and thus the mean spike rate.

From the optimal Kolmogorov–Wiener linear filter, one can estimate the stimulus from the spike train [7,10]. The deviation of this linear estimate from the actual signal defines a mean square error value  $\varepsilon$ . The filter is chosen such that it minimizes this mean square error. The coding fraction  $\kappa$  is a normalized measure of the quality of the linear reconstruction achieved by the cell:

$$\kappa = 1 - \frac{\varepsilon}{\sigma}, \quad (8)$$

where  $\sigma$  is the variance of the stimulus. To calculate coding fraction, MatLab code from Gabbiani [7,11,12] was

used. It uses as input the original stimulus (the low-pass filtered Gaussian noise) and a binary representation of the spike train generated by the LIF model with synaptic dynamics.

## 4. Results

### 4.1. Filtering properties

While examining filtering properties, we dissected our system according to different variables, and individually studied the separate stages. The detailed description of these results is beyond this paper. We found that the depression dynamics is able to act as a low or band-pass filter, depending on the ratio  $\tau_d/\tau_g$  between the time constants of recovery from depression ( $\tau_d$ ) and decay of the synaptic conductance ( $\tau_g$ ). On increasing the synaptic depression time constant, the overall synaptic conductance decreases but when  $\tau_d$  exceeds  $\tau_g$ , the gain function becomes non-monotonic. The peak of the hump is dependent on the  $\tau_d/\tau_g$  ratio (Fig. 1(A)). In case of further increased  $\tau_d$  (35 ms), the firing rate drop dominates, thus the gain non-monotonicity disappears (Fig. 1(A)). In order to closer investigate the physiological parameters of our system, we fixed the recovery time constant of the depression to be  $\tau_d = 15$  ms. This corresponds well with recovery time constants found in other systems transmitting high frequencies [3]. With this fixed  $\tau_d$  we ran further simulations where now we changed the time constant of the synaptic conductance  $\tau_g$  and found similar results to our previous ones (not shown). The coherence measure (Fig. 1(B)) changes qualitatively depending on the depression recovery time constant. It also becomes non-monotonic in the parameter regime where  $\tau_d > \tau_g$ .

### 4.2. Dependence of coding properties on synaptic dynamics

Next we compared the coding capabilities of the postsynaptic neuron while changing the time constants of the synaptic dynamics. While studying the sensitivity of the coding properties to  $\tau_d$  and  $\tau_g$ , we had to take into account the firing rate change of the LIF, since firing rate affects information transmission [11,12]. We therefore used the following two methods [11,12]: (A): *Mutual information per spike* was used. For spike train generation, we used A-type LIF simulations (see Methods); (B): the postsynaptic cell's firing rate change was compensated via DC current injection, in order to keep it at the same mean value (B-type simulations).

The low coding fraction values agree well with earlier results reported in similar doubly stochastic models, where for an ideal deterministic single synapse with high input stimulus bandwidth ( $> 50$  Hz), the coding fraction values were less than 0.1 [8]. We found that, as the synaptic depression recovery time constant increased, the coding fraction decreased (Fig. 1(E)). The *mutual information per spike* measure however increases (Fig. 1(C)). This is due to

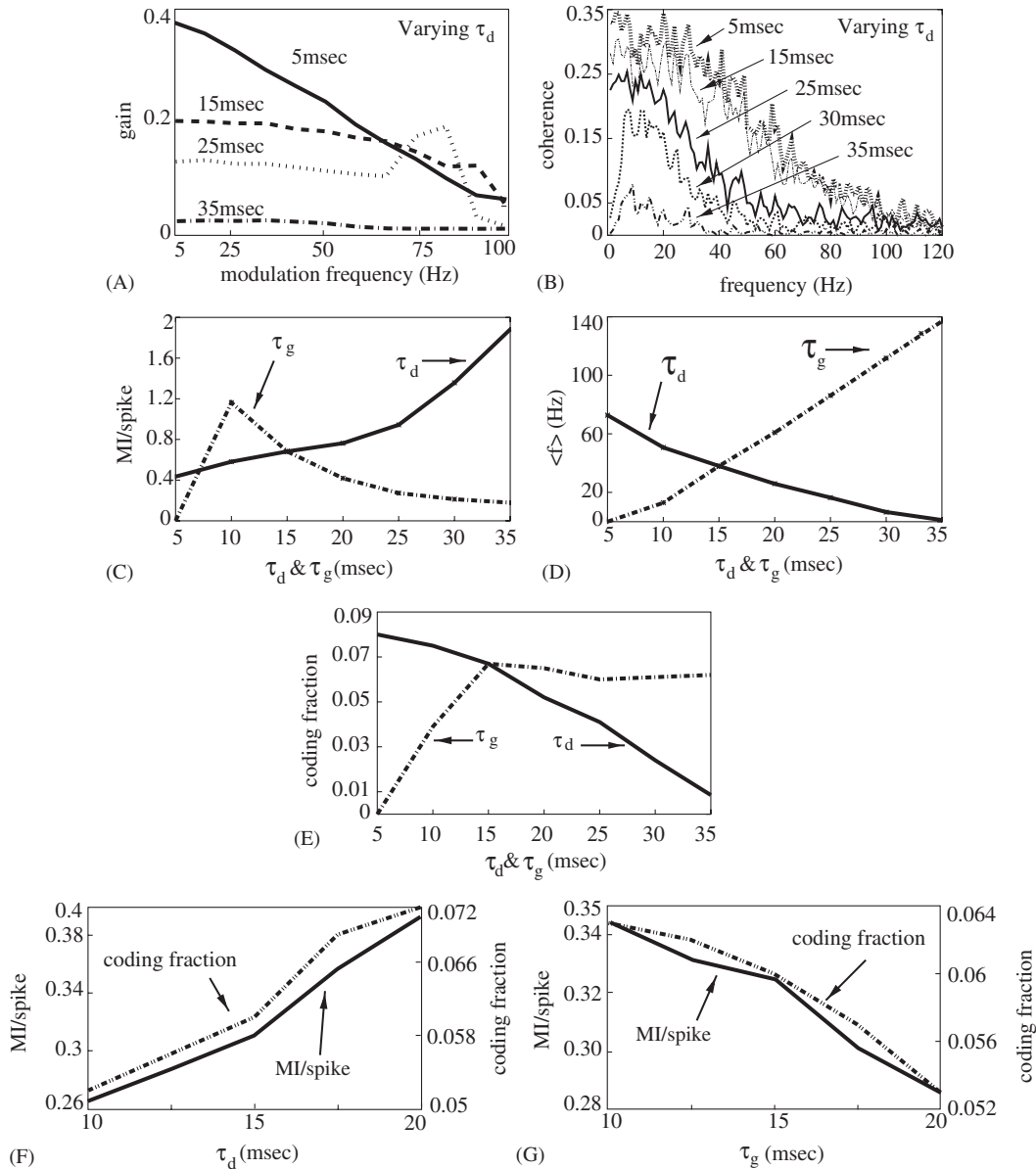


Fig. 1. (A) Gain curve obtained for the LIF neuron for the sinusoidally modulated Poisson input without controlling for firing rate (Methods—type A simulations for panels A–E). The synaptic recovery time constant  $\tau_d$  is varied, while keeping  $\tau_g = 15$  ms constant. (B) Coherence curves between the input noise stimulus and output spike train while varying  $\tau_d$  and keeping  $\tau_g = 15$  ms constant. (C) Mutual information per spike and (E) coding fraction as a function of  $\tau_d$  and  $\tau_g$ . (D) Mean firing rate of the LIF neuron as a function of  $\tau_d$  and  $\tau_g$ . While varying one time constant, we kept the other time constant fixed. (F) Mutual information rate per spike and (G) coding fraction as a function of  $\tau_d$  and  $\tau_g$ . For panels F–G, while changing  $\tau_d$  we kept  $\tau_g = 10$  ms, and while changing  $\tau_g$ ,  $\tau_d$  was kept constant at 15 ms. Also, the postsynaptic firing rate  $\langle f \rangle$  was fixed (at  $\approx 72$  Hz) for panels F–G (type B simulations).

the fact that, despite the firing rate drop (Fig. 1(D)), the cell fires more reliably to stimulus upstrokes, due to the depression dynamics. The coding fraction drop with increasing  $\tau_d$  (Fig. 1(E)) parallels the decreasing firing rate (Fig. 1(D)), as found in earlier studies [8,12].

Next, the synaptic depression time constant was fixed (15 ms), and we varied the synaptic conductance time constant. The firing rate increased with longer synaptic inputs (larger  $\tau_g$ —Fig. 1(D)), as expected. The *mutual information per spike* decreased with  $\tau_g$  (Fig. 1(C)); the

timing of the postsynaptic firing becomes less reliable as the synaptic event is longer. The observed non-monotonicity in Fig. 1(C) is an artifact: at very short  $\tau_g$  values, the synaptic events are not long enough to induce firing (Fig. 1(D)). Thus, MI/spike values start at zero. When the cell starts to fire, the MI/spike values are high, and this value gradually decreases (Fig. 1(C)). The coding fraction has a slight non-monotonicity because the postsynaptic firing becomes less precise but the linear reconstruction improves with firing rate increase (Fig. 1(E)) [12].

To further investigate the synaptic information transmission, the firing rate drop induced by changes in  $\tau_d$  and  $\tau_g$  was compensated by adding a DC current such that the postsynaptic mean firing rate was kept at 72 Hz (Fig. 1(F,G)). Here, we found that both the MI/spike and the coding fraction values change in parallel: with increasing  $\tau_d$ , both increase, and with increasing  $\tau_g$ , both decrease (Fig. 1(F,G)). Thus, with increasing  $\tau_d$  the firing rate drops, but since we compensated this with an increasing DC current, the MI/spike measure increases, although it reaches lower values than on Fig. 1(C). The spiking becomes less precise with increasing  $\tau_g$  (Fig. 1(G)), and this can be followed with both the MI/spike and the coding fraction measures.

## 5. Discussion

A thorough in vitro analysis of the afferent pathway in the ELL revealed NMDA and AMPA components of the excitatory glutamatergic afferent synapses as well as truncating and shunting effects of the GABA-ergic feed-forward inputs on the EPSP shape [2]. Behavioral and in vivo results show that the pyramidal cells in the ELL reliably detect high frequencies in their EOD amplitude modulation [4]. In vivo responses from the ELL pyramidal cells to SAMs show that a subpopulation of the ELL pyramidal cells (E cells) are best described as “receptor like”, thus having high-pass characteristics [9], with peak responsiveness at EOD amplitude modulation frequencies between 32 and 64 Hz [1]. Our simulation results suggest, that in order to see such characteristics the synaptic depression time constant ( $\tau_d$ ) should be longer than the time constant of the synaptic conductance ( $\tau_g$ ). Indeed Fig. 1(A,B) shows that this configuration is capable of band-pass filter characteristics, and high frequency inputs can then be transmitted. According to our simulation results, if NMDA receptors ( $\tau_g > 20$  ms) contribute strongly to the synaptic current, then shorter values for the synaptic depression recovery time will result in a synaptic low-pass filter [2]. In order to preserve gain at higher frequencies, faster AMPA receptor currents, which decay rapidly as seen in vitro [2], should dominate the synaptic response. Under these conditions however the overall gain is decreased (Fig. 1(A)).

Our results on coding ability performance in the signal estimation paradigm correspond well with previous studies on single deterministic synapses [8] submitted to modulated

Poisson input. We have found that increasing  $\tau_d$  in turn increases the information transmitted by single spikes, in spite of a concomitant overall firing rate and coding fraction drop. Coding fraction however parallels the information per spike when one controls for the firing rate. Future work will better constrain model parameters to quantitatively reproduce both filtering and coding properties seen in vivo and in vitro, and investigate how synaptic facilitation may also play a role in this context.

## Acknowledgments

This work was supported by a CIHR grant to L. M. and A. L., and by the NATO Science Fellowship to K. Sz.

## References

- [1] J. Bastian, The effects of moving objects and other electrical stimuli on the activities of two categories of posterior lateral line lobe cells in *Apteronotus albifrons*, *J. Comparative Physiol. A* 144 (1981) 481–494.
- [2] N. Berman, L. Maler, Inhibition evoked from primary afferents in the electrosensory lateral line lobe of the weakly electric fish (*Apteronotus leptorhynchus*), *J. Neurophysiol.* 80 (6) (1998) 3173–3196.
- [3] S. Brenowitz, L.O. Trussell, Minimizing synaptic depression by control of release probability, *J. Neurosci.* 21 (6) (2001) 1857–1867.
- [4] M.J. Chacron, B. Doiron, L. Maler, A. Longtin, J. Bastian, Non-classical receptive field mediates switch in a sensory neuron’s frequency tuning, *Nature* 26 (424) (2003) 1018–1022.
- [5] F.S. Chance, S.B. Nelson, L.F. Abbott, Synaptic depression and the temporal response characteristics of V1 cells, *J. Neurosci.* 15;18 (12) (1998) 4785–4799.
- [6] J.J. Eggermont, The magnitude and phase of temporal modulation transfer functions in cat auditory cortex, *J. Neurosci.* 19 (7) (1999) 2780–2788.
- [7] F. Gabbiani, C. Koch, Chapter in *Methods in Neural Modeling: From Synapses to Networks*, MIT Press, Amsterdam, 1998.
- [8] A. Manwani, C. Koch, Detecting and estimating signals over noisy and unreliable synapses: information-theoretic analysis, *Neural Comput.* 13 (2000) 1–33.
- [9] M.E. Nelson, Z. Xu, J.R. Payne, Characterization and modeling of P-type electrosensory afferent responses to amplitude modulations in a wave-type electric fish, *J. Comp. Physiol.* 181 (1997) 532–544.
- [10] F. Rieke, D. Warland, R. de Ruyter van Steveninck, W. Bialek, *Spikes; Exploring the Neural Code*, MIT Press, Cambridge, MA, 1996.
- [11] M. St-Hilaire, A. Longtin, Comparison of coding capabilities of Type I and Type II neurons, *J. Comput. Neurosci.* 16 (3) (2004) 299–313.
- [12] R. Wessel, C. Koch, F. Gabbiani, Coding of time-varying electric field amplitude modulations in a wave-type electric fish, *J. Neurophysiol.* 75 (6) (1996) 2280–2293.
- [13] S.H. Wu, C.L. Ma, Contribution of AMPA, NMDA, and GABAA receptors to temporal pattern of postsynaptic responses in the inferior colliculus of the rat, *J. Neurosci.* 24 (19) (2004) 4625–4634.



**Krisztina Szalisznyó** received her MD in 1997 from Pécs University Medical School, and her Ph.D. in 2000 from Eötvös Loránd University in Computational Neuroscience. She was a post-doctoral fellow at New York University between 2001 and 2002, and received a NATO science postdoctoral fellowship in 2003–2005 at Ottawa University. Currently, she is a research fellow at the Budapest Computational Neuroscience group.



**Len Maler** received his undergraduate degree at McGill University and his Doctorate in Brain Sciences at the Massachusetts Institute of Technology. While a graduate student he developed an interest in the sensory physiology of electric fish. After postdoctoral fellowships at the Scripps Institute of Oceanography (Ted Bullock) and the Max Planck Institute, he accepted a position at the University of Ottawa. His work has focused on control of information flow by synaptic dynamics and feedback networks.



**Andre Longtin** graduated with a B.Sc. in Physics in 1983, and a M.Sc. Physics (theoretical biophysics) in 1985 from the Université de Montréal. He obtained his Ph.D. in Physics from McGill University in 1989 in theoretical and experimental nonlinear dynamics. He was an NSERC postdoctoral fellow in the Theoretical Division at Los Alamos National Laboratory (Complex Systems Group and Center for Nonlinear Studies) until 1991. He is now Professor of Physics and cross-appointed to the Department of

Cellular and Molecular Medicine at the University of Ottawa, where he co-directs with Len Maler the Center for Neural Dynamics and Computation.